MOLECULAR AND CELLULAR NEUROSCIENCES 3, 64–78 (1992)

Localization of Hypoxanthine-Guanine Phosphoribosyltransferase mRNA in the Mouse Brain by *in Situ* Hybridization

H. A. JINNAH,* E. J. HESS,† M. C. WILSON,† F. H. GAGE,* AND T. FRIEDMANN‡

*Departments of *Neurosciences and ‡Pediatrics, University of California San Diego School of Medicine, La Jolla, California 92093; and †Department of Neuropharmacology, Research Institute of Scripps Clinic, La Jolla, California 92037*

Received for publication October 3, 1991

Congenital deficiency of the purine salvage enzyme hypoxanthine–guanine phosphoribosyltransferase (HPRT) in humans results in a severe neurogenetic disorder known as the Lesch–Nyhan syndrome. Since little information concerning the precise localization of HPRT in the brain is currently available, we have used *in situ* hybridization to examine the expression of HPRT mRNA in the mouse brain. The results showed that HPRT mRNA is expressed in many regions of the normal mouse brain, with high levels in most, but not all neurons. In contrast, glial cells did not express detectable levels of HPRT mRNA. No HPRT mRNA was detected in the brains of mutant mice carrying a deletion in the HPRT gene.

INTRODUCTION

Hypoxanthine–guanine phosphoribosyltransferase (HPRT; EC 2.4.2.8) is an enzyme involved in the salvage pathway for purines. This enzyme catalyzes the conversion of the purine bases hypoxanthine and guanine into inosine monophosphate (IMP) and guanosine monophosphate (GMP), respectively. In the absence of HPRT, hypoxanthine and guanine obtained from exogenous sources or generated during purine metabolism are not incorporated into the cellular purine nucleotide pools, but are degraded and excreted. Although most cells can survive, grow, and function without recycling hypoxanthine or guanine, it is thought that HPRT provides for more economical functioning in the purine metabolic pathways. Therefore, HPRT is normally present as a so-called "housekeeping" enzyme in most mammalian cells.

Although most cells express HPRT constitutively, not all tissues contain equivalent amounts of HPRT enzyme activity. In humans (1–3), rhesus monkeys (4), and mice (5, 6), enzyme assays of tissue extracts have indicated that the brain expresses considerably higher levels of HPRT than other tissues. Furthermore, different regions of the human brain exhibit different levels of HPRT activity, with the highest levels occurring in the basal ganglia (1–3). The high levels of HPRT activity in the brain suggest that the brain, or possibly particular subregions, may be more dependent on purine recycling than other organs.

The importance of purine recycling in the brain is dramatically illustrated by the Lesch–Nyhan syndrome (LNS), an X-linked genetic disorder caused by HPRT deficiency in humans (7, 8). Patients with this disorder exhibit a number of neurobehavioral abnormalities including choreoathetosis, muscular hypotonia with intermittent spasticity, mental retardation, and compulsive aggressive and self-injurious behavior (3, 9–11). Although the mechanisms by which HPRT deficiency lead to the neurobehavioral disturbances remain unclear, several studies have indicated that an abnormality of dopamine transmission in the basal ganglia may play a role. Biochemical studies of the basal ganglia and CSF of patients with this disorder have revealed significant reductions in the levels of dopamine and its metabolites, whereas the levels of other monoamines including norepinephrine and serotonin appear unaffected (12–15). A specific dysfunction of the basal ganglia is also consistent with several elements of the clinical phenotype, such as choreoathetosis, dystonia, and self-injurious behavior, which may be attributable to disturbances of the basal ganglia (16).

Two strains of HPRT-deficient ($HPRT^-$) mutant mice have been produced as animal models for the Lesch–Nyhan syndrome (17, 18). Although these mice do not exhibit the obvious neurobehavioral abnormalities observed in HPRT-deficient humans, they are hypersensitive to drugs that interact with brain dopamine systems, such as amphetamine (19). Also as in patients with Lesch–Nyhan syndrome, the levels of dopamine in the basal ganglia of these mice are significantly reduced (20–23). The high levels of HPRT expressed in the basal ganglia of normal humans, and the relatively specific disturbance of the dopamine systems in the basal ganglia of both HPRT-deficient humans and mice suggests that HPRT plays an important role in the normal functions of this region.

1044-7431/92 $3.00

A more precise definition of the regional and cellular expression of this gene is needed for a better understanding of the behavioral and biochemical abnormalities observed in HPRT-deficient humans and mice. Although the biochemical properties and gross tissue distribution of HPRT in the mouse have been examined (5, 6), no information is currently available concerning the distribution of HPRT in different regions of the mouse brain. Since enzyme measurements of crude extracts from tissue homogenates may obscure important differences in cell-specific patterns of expression, we have used *in situ* hybridization to map the distribution of HPRT mRNA in the brains of normal and HPRT-deficient mice. With this technique, it is possible to analyze the expression of HPRT mRNA directly, at the resolution of single cells.

METHODS

Animals. Mice carrying the HPRT deletion (17) were generously provided by Dr. David Whittingham and maintained congenic with the 129/J or C57BL/6J strains (Jackson Laboratories, Bar Harbor, ME) for at least four generations. Animals were housed in groups of three to five, with a 12-h dark–light cycle and free access to food and water. HPRT-normal ($HPRT^+$) and HPRT-deficient ($HPRT^-$) animals were identified by biochemical assay (24) of a 20-μl sample of blood removed from the tail. All animals used in this study were adult males, 12–20 weeks of age.

Southern analysis. DNA samples for Southern blots were extracted from mouse tail. A 2-cm segment was cut from the end of the tail, placed in a 1.5-ml microfuge tube, and stored at −70°C until needed. The sample was then thawed and incubated overnight at 56°C in 700 μl of DNA extraction buffer consisting of 50 μg/ml proteinase K, 100 m*M* EDTA, 100 m*M* NaCl, 1% SDS, and 50 m*M* Tris buffer, pH 8.0. Protein and other contaminating materials were removed from the mixture by extracting 3× with phenol, 1× with phenol/chloroform, and 1× with chloroform/isoamyl alcohol. The DNA remaining in the mixture was then precipitated by adding 2 vol of ethanol. After a minimum of 60 min at 4°C with gentle mixing, the precipitated DNA was spooled onto a pipette tip and resuspended in 100 μl of 10 m*M* Tris buffer, pH 8.0, containing 1 m*M* EDTA. The DNA was quantified by measuring the 260 uv absorbance; the typical yield from this procedure was 100–125 μg of high molecular weight genomic DNA with a 260/280 ratio of 1.85.

Genomic DNA was digested with restriction enzymes by established procedures (25). Approximately 10 μg of digested DNA was electrophoresed in a 0.9% agarose gel and blotted onto Nytran membrane (Schleicher & Schuell, Keene, NH) using a Vacublot apparatus (Pharmacia LKB Biotechnology, Piscataway, NJ). The DNA was then covalently fixed to the membrane by uv irradiation according to established procedures (25). A ^{32}P-labeled DNA probe for HPRT (sp act, approximately 1×10^9 cpm/μg) was prepared by the random primer method (Multiprime kit from Amersham, Arlington Heights, IL). A 1.2-kb *Pst*I fragment from the plasmid pHPT5 (26) served as the template. It contains the full HPRT coding region as well as several hundred base pairs of noncoding sequence.

Northern analysis. RNA for Northern blots was isolated from tissue samples by a modification of previously described methods (27). A whole brain was homogenized with a Brinkmann Polytron in 5 ml of RNA extraction buffer (4 *M* guanidine thiocyanate, 25 m*M* sodium citrate, pH 7.0, 0.5% Sarcosyl, and 0.1 m*M* β-mercaptoethanol). The following were then added to the mixture with mixing at each step: 500 μl 2 *M* sodium acetate, pH 4.0, 5 ml phenol, 1 ml chloroform/isoamyl alcohol. After 60 min on ice, the mixture was centrifuged in a swinging bucket rotor for 20 min at 25,000*g*. The aqueous phase containing the RNA was then transferred to a new tube containing 5 ml isopropyl alcohol, and RNA was allowed to precipitate overnight at 4°C. The precipitated material was sedimented by centrifugation for 20 min at 1500*g* and resuspended in 500 μl fresh RNA extraction buffer. Some contaminants remaining in the sample were further extracted at this stage with phenol/chloroform and chloroform/isoamyl alcohol. The RNA was then precipitated a second time with 500 μl isopropanol. After centrifugation, the pellet was resuspended in distilled water, quantitated by 260 uv absorbance, and stored at −70°C until further use.

An aliquot of 10 μg of total RNA was electrophoresed on a 1.2% agarose/formaldehyde gel, blotted onto Nytran membrane, and covalently fixed by uv irradiation as described above. The membrane was then probed with the same probe used for Southern analysis. The RNA content was standardized by reprobing blots with probes for rat cyclophilin (28), mouse APRT (29), or avian β-actin (30).

Tissue preparation. Mice were anesthetized with CO_2 and perfused through the heart with approximately 25 ml of 0.9% saline, followed by 100 ml of a freshly prepared fixation solution of 4% paraformaldehyde in 0.1 *M* phosphate buffer, pH 7.5. After perfusion, the brain and spinal cord were removed and immersed in the same fixative for 3–8 h. The tissue was then equilibrated in 16% glucose for 16 to 24 h and cut at a thickness of 20 μm on a cryostat.

Sections from normal and $HPRT^-$ mice were processed under identical conditions. Matched sections from one normal and one mutant animal were mounted together on the same slide, and a series of slides containing sections from the whole brains of the two animals were processed together. A total of six normal and six $HPRT^-$ mice was used to establish the regional distribution of HPRT mRNA.

In situ hybridization. *In situ* hybridization was performed as previously described, using ^{35}S-labeled RNA

probes (31). The template for transcription of the HPRT probes was created by subcloning a 1.2-kb *Pst*I fragment containing the entire mouse HPRT cDNA from the plasmid pHPT5 (26) into pGEM3 (Promega Biotec, Madison WI), generating the plasmid pMHG. The template for transcription of the cyclophilin probes was created by subcloning a 950-bp *Bam*HI fragment containing the entire rat cyclophilin cDNA from the plasmid p1B15 (28) into GEM3, generating the plasmid pMAG. Antisense and sense probes for both HPRT and cyclophilin were transcribed by SP6 and T7 RNA polymerases, respectively. After *in vitro* transcription, the DNA template was removed by digestion with RNase-free DNase (Promega Biotec, Madison, WI), and the size of the transcripts was reduced to 150–250 nucleotides by alkali treatment.

Pretreatment of the slide-mounted sections included fixation in buffered 4% formaldehyde for 5 min at room temperature, followed by treatment with 25 μg/ml proteinase K in 50 m*M* Tris, pH 8.0, and 5 m*M* EDTA for 7.5 min at 37°C, treatment in 0.5 *N* HCl for 7.5 min at room temperature, and a final 5-min postfixation in buffered 4% paraformaldehyde. Slides were rinsed 2 × 2 min in PBS between each of the aforementioned steps. Sections were then dehydrated in graded concentrations of ethanol and air-dried. Slides were incubated at 52°C for 2–3 h in approximately 750 μl of a prehybridization buffer containing 50% formamide, 0.75 *M* NaCl, 20 m*M* Pipes buffer, pH 6.8, 10 m*M* EDTA, 10% dextran sulfate, 5× Denhardt's solution (0.02% BSA, 0.02% Ficoll, 0.02% polyvinylpyrolidone), 50 m*M* DTT, 0.2% SDS, 100 μg/ml salmon sperm DNA, and 100 μg/ml yeast tRNA. Prehybridization buffer was removed from the slides and 75 μl of hybridization solution consisting of prehybridization buffer plus 10–15 ng ^{35}S-labeled RNA probe (sp act, approximately 6.6×10^8 cpm/μg) was applied to each slide. Slides were covered with coverglass and allowed to hybridize for 16 h at 52°C.

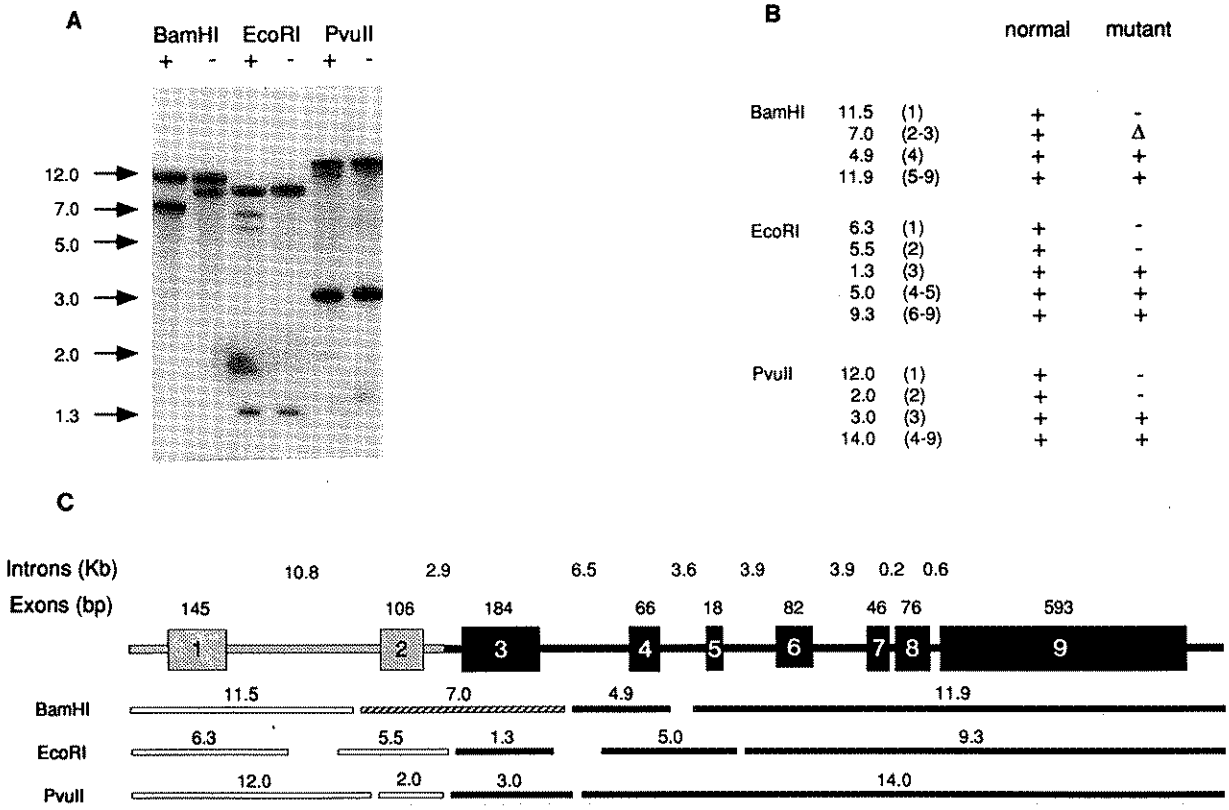

FIG. 1. Molecular analysis of the HPRT gene in mice with HPRT deficiency. (A) Southern analysis of DNA samples from normal (lanes labeled "+") and mutant (lanes labeled "−") mice. Genomic DNA was isolated from tail; digested with *Bam*HI, *Eco*RI, or *Pvu*II; and electrophoresed on a 0.9% agarose gel. DNA in the gel was then blotted onto Nytran membrane, and the membrane was hybridized with a ^{32}P-labeled DNA probe for the entire HPRT cDNA. (B) Summary table of restriction fragments observed in normal and HPRT-deficient mice. The restriction fragment sizes expected for the normal mouse HPRT gene are shown for each enzyme, followed in parentheses by the exons they contain (33, 34). Hybridizing bands are indicated by a plus; absences are indicated by a minus, and changes in size are indicated by a Δ. (C) Schematic representation of the mutation carried by the HPRT-deficient mice. The nine exons of the normal HPRT gene are shown as large boxes, together with the sizes of introns and exons (33, 34). Restriction sites and fragment lengths for *Bam*HI, *Eco*RI, and *Pvu*II are shown below the gene. The promotor region and first two exons of the gene (shown as grey boxes) appear to be deleted in the HPRT-deficient mice.

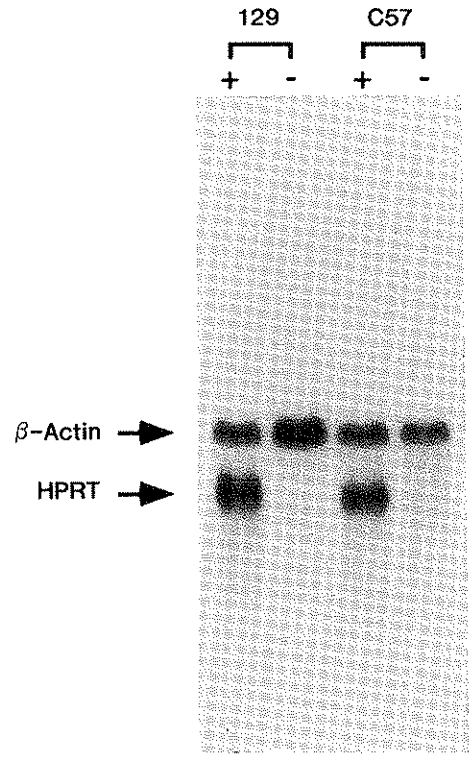

FIG. 2. Northern blot analysis of RNA samples extracted from the brains of normal (lanes labeled "+") and HPRT$^-$ (lanes labeled "–") mice. Ten micrograms of total RNA was electrophoresed on a 1.2% agarose/formaldehyde gel and blotted onto Nytran membrane, and the membrane was hybridized with a ^{32}P-labeled DNA probe for HPRT and β-actin (30). The bands resulting from hybridization with the β-actin probe reveal that similar amounts of RNA were loaded in each lane; however, HPRT mRNA could not be detected in samples from HPRT$^-$ mice, even after prolonged exposure of the blot (not shown).

Following hybridization, coverslips were removed and the slides were rinsed briefly in 0.15 *M* NaCl with 0.015 *M* sodium citrate and 300 m*M* β-mercaptoethanol at room temperature, followed by a 15-min rinse in the same solution without β-mercaptoethanol at room temperature. Sections were treated with 50 μg/ml pancreatic RNase A in 0.5 *M* NaCl, 50 m*M* Tris, pH 8.0, 5 m*M* EDTA for 30 min at 37°C; rinsed for 30 min at 37°C in this same buffer; washed in 75 m*M* NaCl with 7.5 m*M* sodium citrate at 56°C for 15 min; and air-dried. Sections were exposed to Cronex X-ray film (DuPont, NY) for 2–4 days. They were then dipped in Kodak NTB-2 photographic emulsion diluted 1:2 with distilled H_2O and exposed at 4°C for 7–10 days.

RESULTS

Molecular Characterization of an HPRT-Deficient Mouse

The HPRT-deficient mice used in this study were produced from embryonal stem cells carrying a deletion spanning the 5′ end of the HPRT gene (17, 32). After maintaining the animals congenic with either the C57BL/6J or 129/J strains for at least four generations, it was important to verify that the original mutation had not undergone further modification by recombination or additional mutations. Therefore, the HPRT gene was examined by Southern analysis of genomic DNA from normal and mutant mice. DNA was digested with the restriction enzymes *Pvu*II, *Eco*RI, and *Bam*HI and probed with a full-length cDNA of the HPRT gene (Fig. 1A). Since some of the bands are only faintly visible on this exposure of the blot, a summary of the restriction fragments expected from previous analyses of normal mice (33, 34) and the fragments observed in mutant animals is presented in tabular form (Fig. 1B). In *Pvu*II digests, the 12-kb band containing exon 1 and the 2-kb band containing exon 2 are absent from the genomic DNA of HPRT$^-$ mice. By contrast, the 3-kb band containing exon 3 and the 14-kb band containing exons 4–9 appear normal. These results suggest that exons 1 and 2 have been deleted in the HPRT$^-$ mice, leaving the remainder of the gene largely intact. These results are corroborated by *Eco*RI digests, in which the 6.3-kb band containing exon 1 and the 5.5-kb band containing exon 2 are both absent, whereas the 1.3-kb band containing exon 3, the 5.0-kb band containing exons 4–5, and the 9.3-kb band containing exons 6–9 are not altered. In *Bam*HI digests of HPRT$^-$ mouse DNA, the 7.0-kb band containing exons 2 and 3 is replaced by a 9.5-kb band containing only exon 3. These restriction fragments indicate the occurrence of a deletion that includes the first two exons of the gene as well as several kilobases of upstream sequence (Fig. 1C). The same mutation was found in both C57BL/6J and 129/J mice carrying the mutant gene and appears identical to that described for the embryonal stem cells from which the mice were originally produced (17, 32).

Since the deletion includes the promotor as well as the first two exons of the gene, it is unlikely that HPRT mRNA could be transcribed in the HPRT$^-$ mice. Results from Northern analysis of RNA extracted from the brains of normal and HPRT$^-$ mice are shown in Fig. 2. Normal and mutant mice expressed nearly identical levels of other housekeeping mRNAs such as β-actin (Fig. 2), adenine phosphoribosyltransferase (APRT), and cyclophilin (results not shown). However, HPRT mRNA was not detected in tissues from HPRT$^-$ mice. These results demonstrate the specific absence of detectable HPRT mRNA in the brains of the HPRT$^-$ mice.

In Situ Hybridization Controls

The availability of mice that do not express HPRT mRNA provides a unique negative control to determine the specificity of *in situ* hybridization studies for HPRT. As shown in Fig. 3, hybridization of a ^{35}S-labeled antisense riboprobe of a full-length HPRT cDNA with sections from

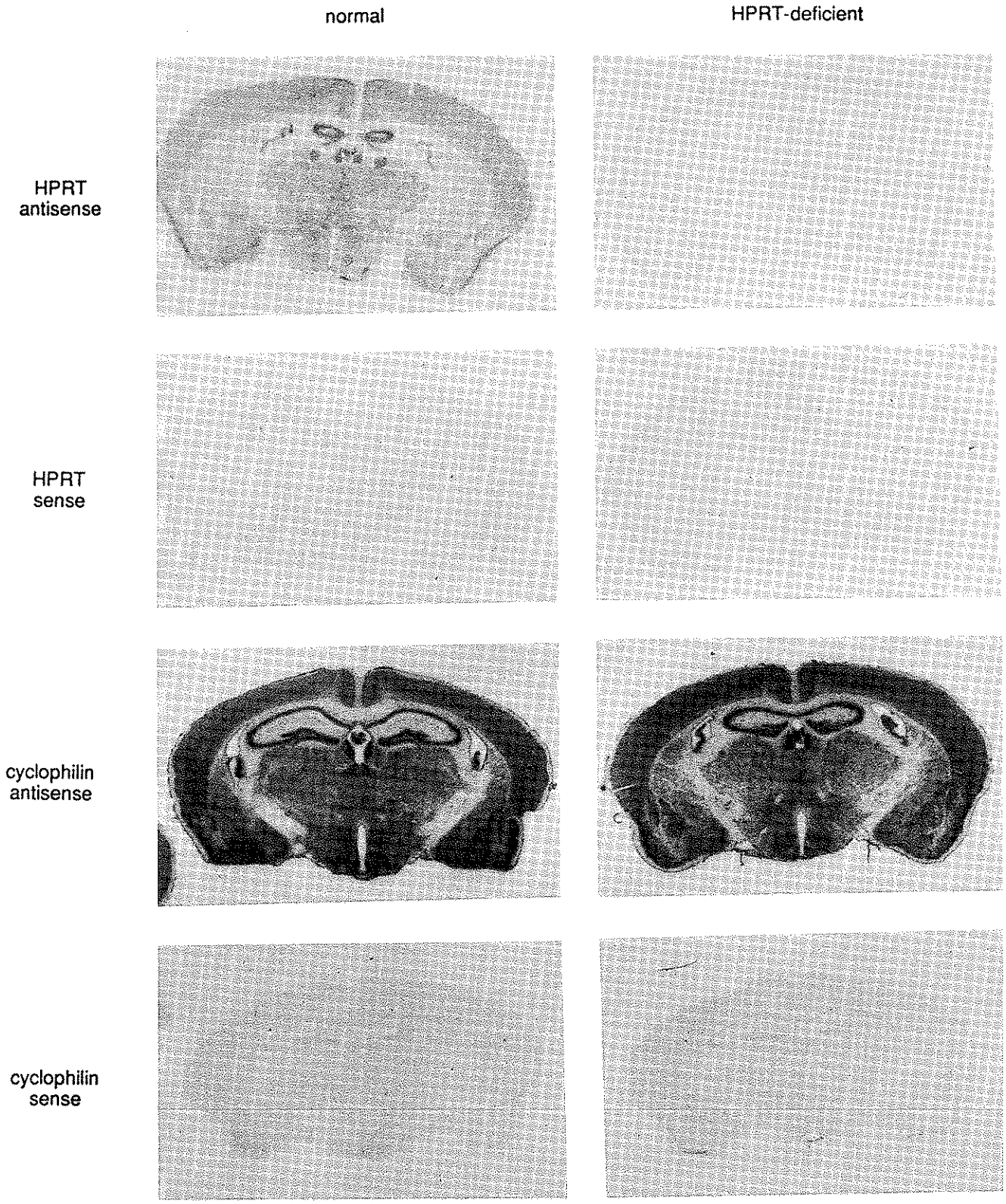

FIG. 3. Controls for HPRT *in situ* hybridization. Tissue sections from normal mice are shown on the left; tissue sections from HPRT$^-$ mice are shown on the right. Sections were hybridized as described under Methods with ^{35}S-labeled antisense or sense RNA probes for HPRT or cyclophilin and exposed to X-ray film for 2–3 days. Although sections from normal and HPRT$^-$ mice both hybridized with the cyclophilin antisense probe, only sections from normal mice hybridized with the HPRT antisense probe. Control (sense) probes for HPRT and cyclophilin displayed only nonspecific hybridization.

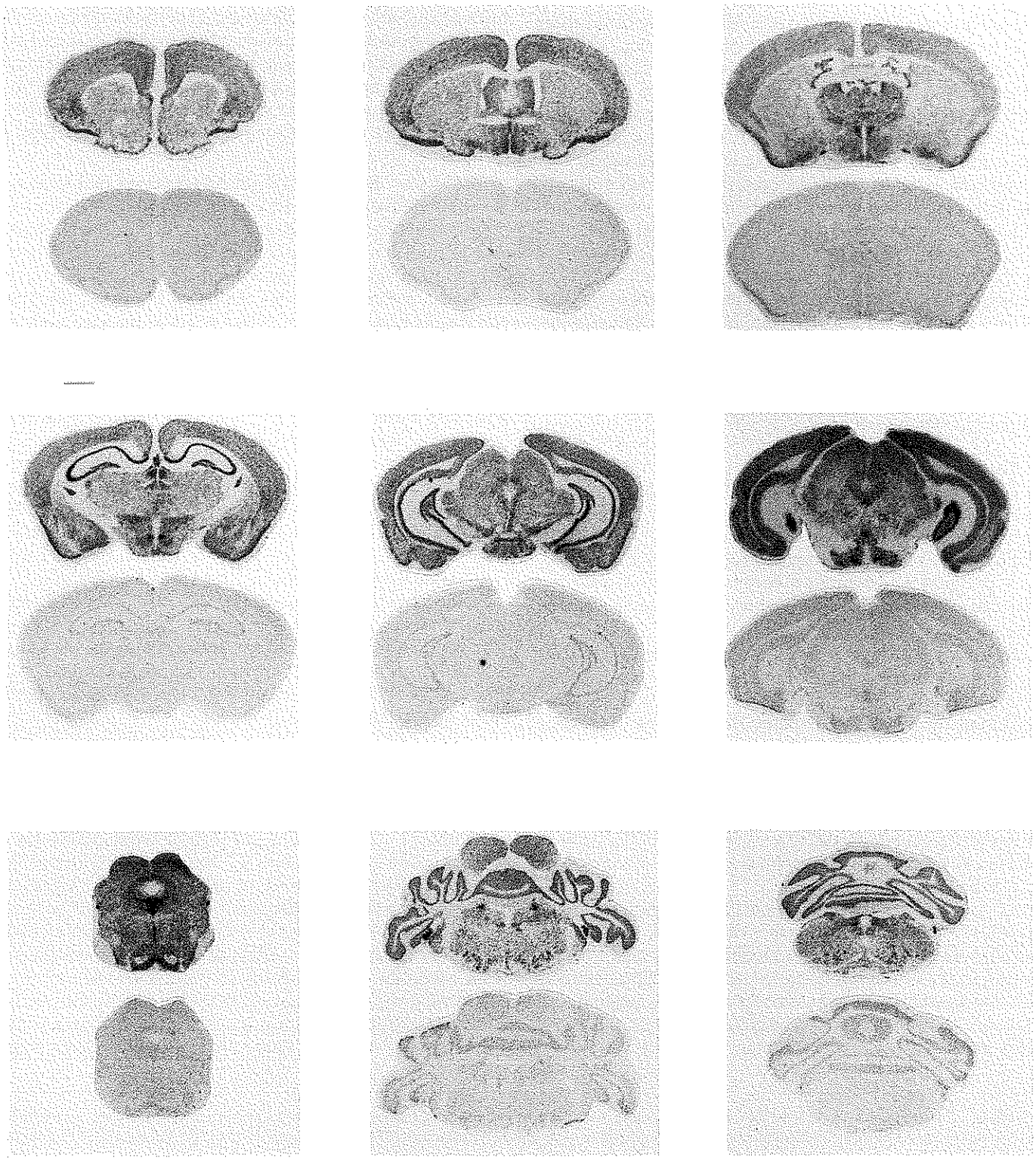

FIG. 4. Regional distribution of HPRT mRNA in sections from the mouse brain. Sections were labeled as described under Methods, with a ^{35}S-labeled antisense RNA probe for HPRT and exposed to X-ray film for 2–3 days. The top image of each pair was obtained from a normal mouse and shows the regional variations in expression of HPRT mRNA in the brain. The bottom image of each pair was obtained from an HPRT-deficient mouse and processed in parallel with sections from normal animals to determine regional variations in the intensity of background hybridization. Although small variations in the intensity of hybridization occurred in different experiments, exposures of sections, film, and photographs were kept as constant as possible.

normal animals showed a distinct pattern of hybridization that was absent in sections from HPRT$^-$ mice. Using a ^{35}S-labeled sense HPRT riboprobe as a control, no specific hybridization was observed in sections from normal or HPRT$^-$ mice (Fig. 3). To verify that the absence of HPRT mRNA in sections from the HPRT$^-$ mice was not a consequence of RNA degradation, *in situ* hybridization was performed using a probe to cyclophilin, a ubiquitously expressed enzyme involved in protein processing (28, 35). Antisense probes for cyclophilin hybridized equally to tissue from normal and HPRT$^-$ mice, while sense probe hybridization for this marker was not detectable (Fig. 3). The results from the *in situ* hybridization studies are consistent with the results from the Northern analysis described above and verify the absence of detectable HPRT mRNA in the brains of the HPRT$^-$ mice.

Regional Distribution of HPRT mRNA

To define the regional distribution of HPRT mRNA in the normal mouse brain, *in situ* hybridization studies were performed on 20-μm sections spaced at approximately 150-μm intervals through the entire rostrocaudal extent of the brain. Matched sections from HPRT$^-$ mice were processed under identical conditions to determine regional differences in nonspecific background labeling. The results are shown in Fig. 4.

Forebrain. In the telencephalon, the strongest hybridization occurred in the mitral and granule cell layers of the olfactory bulb, the pyramidal cell layer of the hippocampal formation, and the piriform cortex. The neocortex, dentate gyrus of the hippocampal formation, and the amygdala also displayed strong hybridization. Hybridization in the caudoputamen and septum was relatively weak, but clearly above background. Hybridization in the corpus callosum and other white matter fiber tracts was not distinguishable from background levels observed in sections from HPRT$^-$ mice.

In the diencephalon, the hypothalamus generally displayed more hybridization with the HPRT probe than the thalamus. Except for the moderate to strong hybridization in the anterodorsal nucleus, the medial habenula, and the thalamic paraventricular nucleus, most of the thalamus showed only weak hybridization. In comparison, most nuclei of the hypothalamus displayed strong hybridization with the HPRT probe. Heavily labeled regions of the hypothalamus included the medial and lateral preoptic areas, the paraventricular nucleus, the lateral hypothalamic area, the suprachiasmatic nucleus, the supraoptic nucleus, the dorsomedial nucleus, the ventromedial nucleus, the arcuate nucleus, and the mammillary complex.

Midbrain. Strongly hybridizing regions of the mesencephalon included the interpeduncular nucleus, the superior colliculus, the periaqueductal grey, the red nucleus, and cranial nerve nuclei III (oculomotor) and IV (trochlear). The subtantia nigra (pars compacta) displayed moderate hybridization to the HPRT probe. Regions containing mostly glial cells and fibers of passage such as the cerebral peduncles and medial lemniscus showed background levels of hybridization.

Hindbrain. The regions of the hindbrain showing the strongest hybridization included the locus coeruleus and the ventral cochlear, pontine, trapezoidal, and raphe nuclei. The large motor neurons of the cranial nerve nuclei also displayed strong hybridization to the HPRT probe, including V (trigeminal), VII (facial), X (vagal), and XII (hypoglossyl). Overall, the brain stem reticular formation was only moderately labeled; but intense clusters of hybridization appeared dispersed throughout the region.

In the cerebellum, the granule and Purkinje cell layers showed strong hybridization, while the molecular layer did not. The cells of the deep cerebellar nuclei also displayed strong hybridization with the HPRT probe. All major white matter fiber tracts demonstrated background levels of hybridization.

Spinal cord. Clusters of dense hybridization to the HPRT probe were observed in the ventral horn. The dorsal horn displayed a diffuse but strong hybridization signal. In contrast, the fiber tracts were not notably labeled.

Summary. A general feature of the whole tissue section autoradiograms is that regions with a high density of neurons displayed much more intense hybridization than regions with lower densities of neurons. This is most obvious in regions such as the dentate gyrus and pyramidal cell layers of the hippocampus or the granule cell layer of the cerebellum, where nearly all of the cells are neurons. In contrast, regions containing high densities of glial cells such as the white matter areas and the glia limitans were not detectably labeled. These observations suggest that

FIG. 5. Distribution of HPRT mRNA as shown by dark-field photomicrographs of emulsion-coated sections. *In situ* hybridization for HPRT mRNA was performed using ^{35}S-labeled riboprobes; the sections were coated with Kodak NTB-2 photographic emulsion, exposed for 7–10 days, and developed. Silver grains, represented by white dots, show areas of probe hybridization. (A) Neocortex. (B) Higher power view of the neocortex showing clustering of silver grains. (C) High power view of neocortex after *in situ* hybridization in a section from an HPRT$^-$ mouse showing background silver grain density. (D) Hippocampal formation. (E) Higher power view of the dentate gyrus and hilar interneurons of the hippocampal formation. (F) Thalamus showing relatively high hybridization in the anterodorsal nucleus. (G) Hypothalamus showing arcuate and ventromedial nuclei. (H) Dense labeling in the piriform cortex, with moderately hybridizing caudoputamen visible in the upper left corner. (I) Olfactory bulb showing heavy hybridization in the mitral and granule cell layers. (J) Spinal cord showing clustering of silver grains over individual motor neurons in the ventral horn and diffuse hybridization in the dorsal horn.

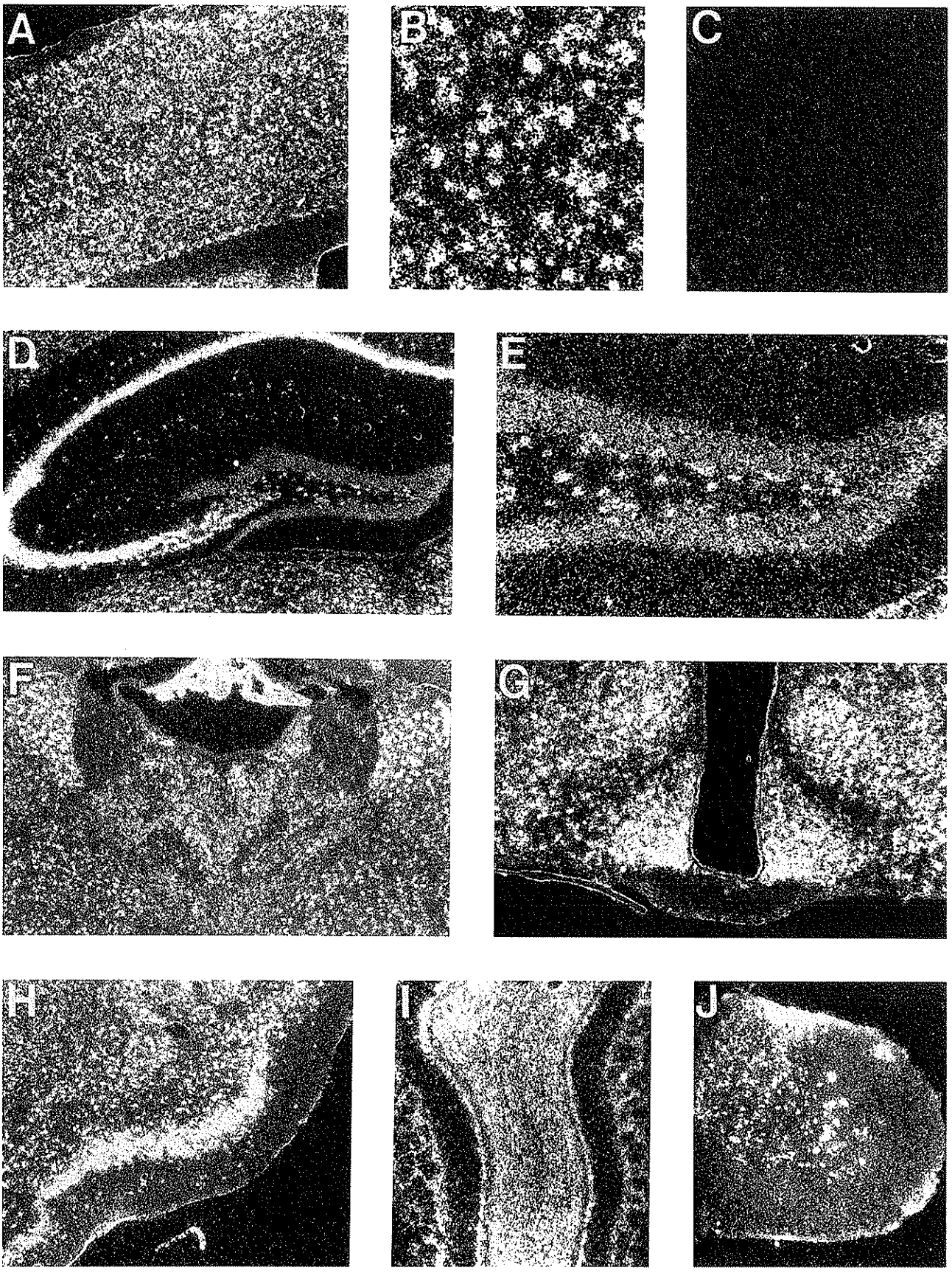
A
B
C
D
E
F
G
H
I
J

HPRT is expressed preferentially in neurons rather than glia. However, in the neuron-dense regions, the intensity of the signal was not necessarily correlated with the cell density as shown by Nissl stains, suggesting that different neurons express different levels of HPRT.

Cellular Resolution of HPRT mRNA Expression

To determine more precisely the cell types expressing HPRT mRNA, sections from the brains of normal and HPRT$^-$ mice were coated with photographic emulsion, exposed for 7–10 days, and developed. With this preparation dense clustering of silver grains could be observed over specific cells. Although the regions such as the piriform cortex, hippocampus, and hypothalamic nuclei displayed the most intense overall hybridization, individual cells in other regions appeared equally if not more intensely labeled. In both dark-field and counterstained bright-field images, the most heavily labeled cells could usually be identified as neurons.

Dark-field microscopy revealed cells with a heavy grain density throughout the brain (Figs. 5–6). In the cortex, silver grains appeared clustered over large diameter cells in all layers (Figs. 5A and 5B). For comparison, dark-field photomicrographs of sections from HPRT$^-$ mice demonstrated a low and random background pattern of silver grains throughout the cortex (Fig. 5C). In the hippocampus, heavily labeled profiles suggestive of individual hilar interneurons could be identified, in addition to neurons of the pyramidal and dentate gyrus cell layers (Figs. 5D and 5E). Dark-field microscopy also revealed a moderate to weak grain density in the substantia nigra pars compacta (Fig. 6A), with a stronger signal in the locus coeruleus (Fig. 6B) and median raphe (Fig. 6C). A heavy grain density was observed over the motor neurons of most cranial nerve nuclei (Figs. 6D–6F). In the cerebellum, silver grains were found distributed throughout the granule and Purkinje cell layers, with slightly higher levels in the latter (Fig. 6G).

Relative differences in the grain density overlying different cells were most obvious in bright-field images of counterstained sections, in which it was common to identify cells with a very high grain density together with other counterstained cells that displayed little or no hybridization to the HPRT probe (Fig. 7). Clearly identifiable cells included the neurons of the lateral vestibular nucleus (Fig. 7A), trigeminal motor nucleus (Fig. 7B), trapezoid body (Fig. 7C), and cerebellar Purkinje cell layer (Fig. 7D). Some of the most heavy grain densities in the entire brain were found over cells in the brain stem reticular formation, a region with a low overall hybridization. These cells displayed the location, size, and shape of the gigantocellular reticular neurons (Fig. 7E).

These results clearly show that not all cells in the brain were labeled with equal intensity. The regional distribution of hybridization and the microscopic analysis of labeled cells demonstrated that neurons expressed substantial levels of HPRT mRNA, while glial elements in the same regions were devoid of detectable levels. However, HPRT was not expressed at uniformly high levels in all neurons, since cells in certain brain regions such as the caudoputamen, basal forebrain, and most of the thalamus appeared to be labeled with a low to moderate intensity.

DISCUSSION

These studies document the relative levels of HPRT mRNA in different regions and cells of the mouse brain. In view of the known housekeeping function of HPRT in intermediate purine metabolism, one might have expected a relatively homogeneous and ubiquitous pattern of expression in all brain cells. On the other hand, the abnormalities of the dopamine systems in HPRT-deficient humans and mice suggest that HPRT may be elevated in the basal ganglia. Surprisingly, neither of these predictions was confirmed. HPRT mRNA was expressed unequally in most neurons, with little or no expression in glial cells.

The pattern of HPRT mRNA expression observed in the autoradiograms of Fig. 4 was similar to previously described patterns for other mRNAs that are expressed exclusively or predominantly in neurons, such as β-amyloid precursor protein (36), the synaptosomal-associated protein SNAP-25 (37), and the vesicle-associated membrane protein VAMP-2 (38). In contrast, the pattern of HPRT mRNA expression differed considerably from that described for glial fibrillary acidic protein (GFAP), which is expressed in astrocytes of the glia limitans and specific white matter regions (39, 40). The pattern of HPRT expression was also considerably different from that of myelin basic protein, proteolipid protein, and myelin-associated glycoprotein, which are expressed in oligodendrocytes of the white matter fiber tracts (41–44). These results suggest that most of the HPRT mRNA found in the brain is expressed by neurons, not glia. Microscopic analysis of counterstained tissue sections confirmed that neurons express considerable levels of HPRT mRNA, while glial cells do not. The absence of detectable HPRT mRNA in areas containing mostly glia does not mean that HPRT is not expressed by these cells, but rather that the level of mRNA in glia was low enough that it was not detected in the current study.

The high levels of HPRT mRNA expressed by some neurons raises a question concerning its function in these cells. In view of the role of HPRT in purine metabolism, it is important to consider the potential involvement of this enzyme in purine-related neurotransmission. Many studies have demonstrated that adenosine and related purines behave as neurotransmitters or neuromodulators in the brain (45–49), and HPRT may play a role in re-

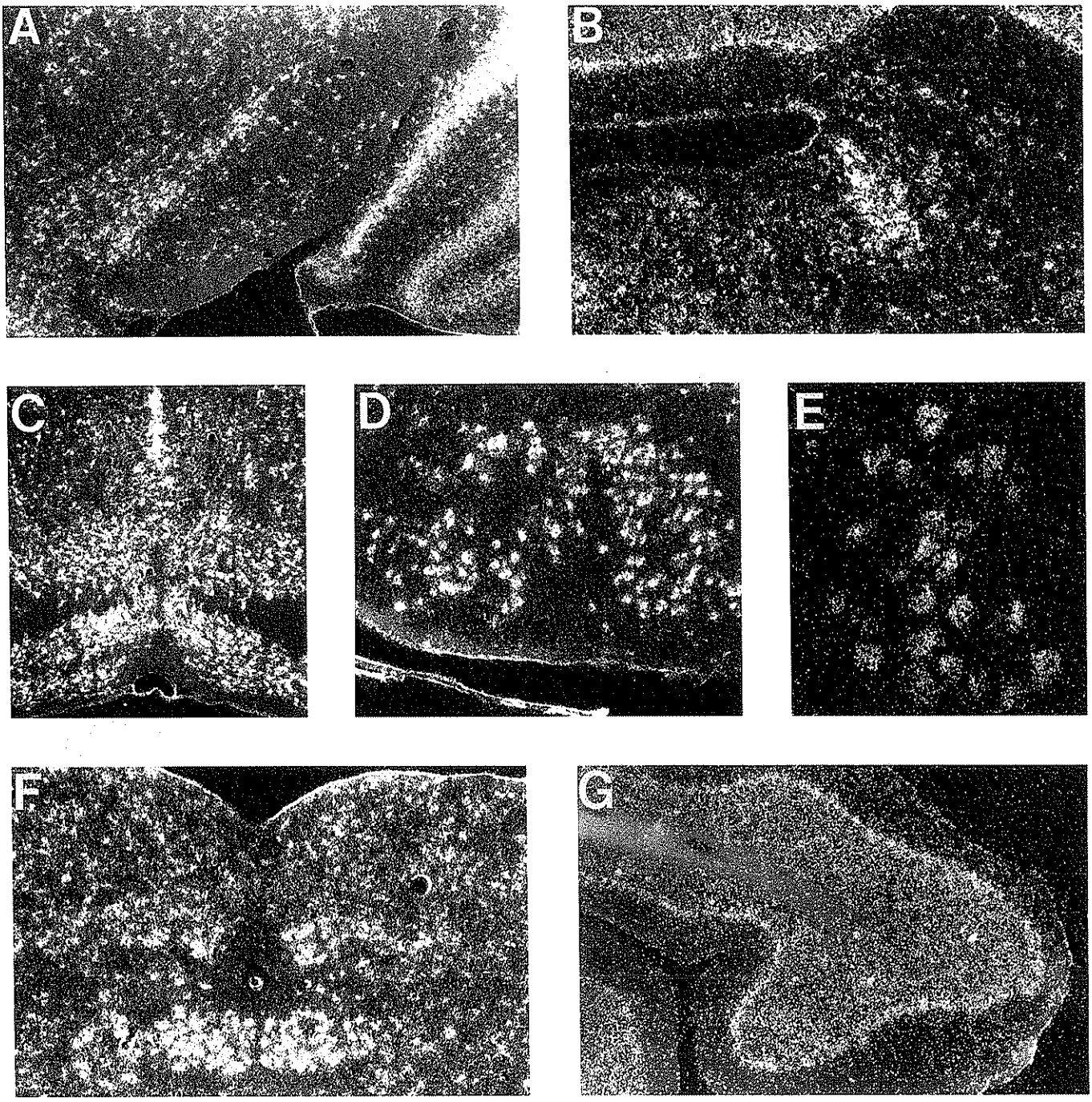

FIG. 6. Distribution of HPRT mRNA as shown by dark-field photomicrographs of emulsion-coated sections. *In situ* hybridization for HPRT mRNA was performed using ^{35}S-labeled riboprobes; the sections were coated with Kodak NTB-2 photographic emulsion, exposed for 7–10 days, and developed. Silver grains, represented by white dots, show areas of probe hybridization. (A) Substantia nigra. (B) Locus coeruleus. (C) Dorsal raphe and Pontine nucleii. (D) Cranial nerve VII (facial nucleus). (E) Higher power view showing motor neurons of the facial nucleus. (F) Motor neurons of cranial nerves X (vagal nucleus) and XII (hypoglossal nucleus). (G) Cerebellum (flocculus) showing labeling of Purkinje and granule cell layers.

cycling these transmitters. Several studies have shown that adenosine released as a neurotransmitter can be metabolized via two different pathways. One pathway involves the reuptake and phosphorylation of adenosine into adenine nucleotides by adenosine kinase (AK pathway), while the other pathway involves enzymatic degradation

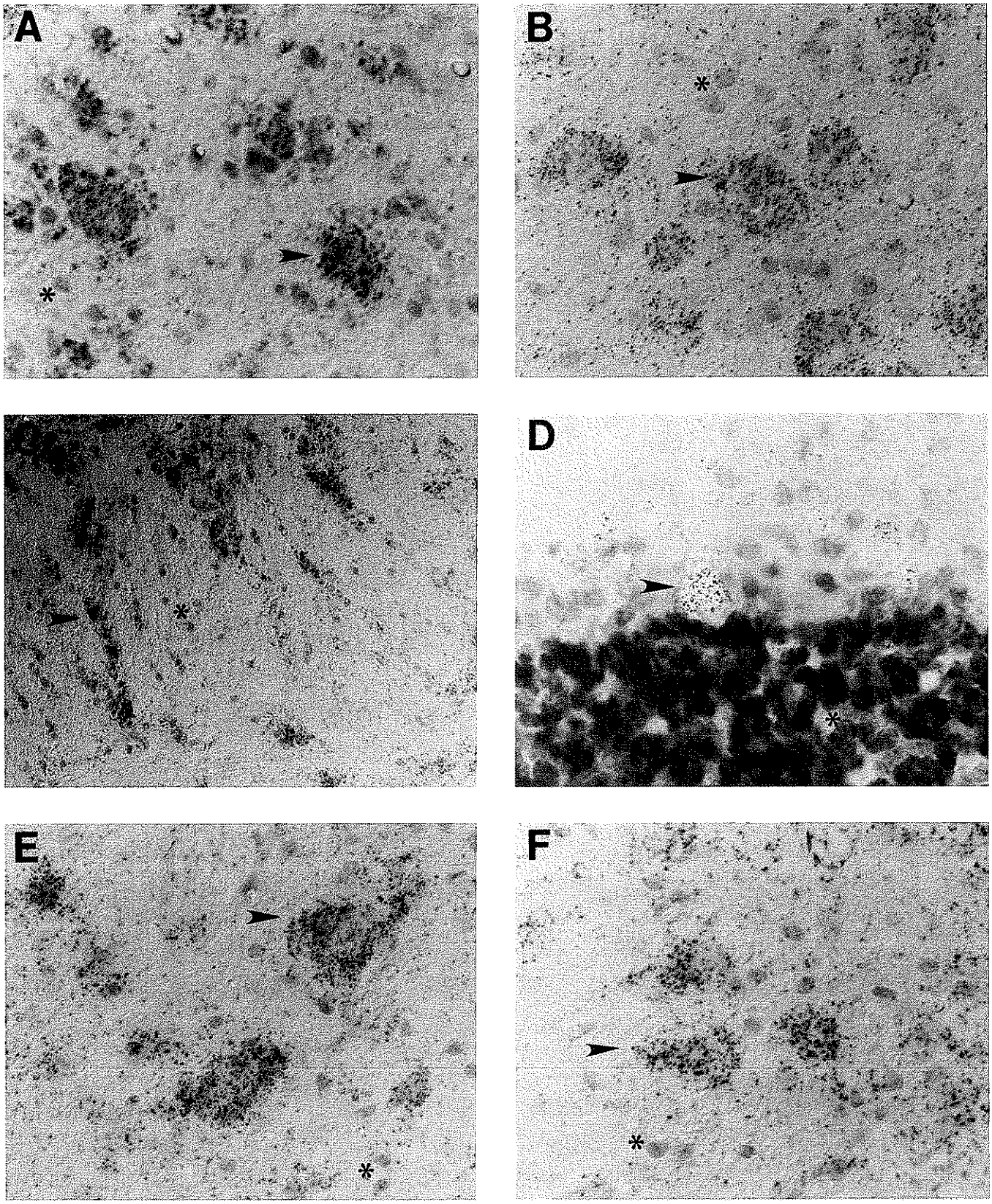

FIG. 7. Cellular localization of HPRT mRNA as shown by counterstained bright-field photomicrographs of emulsion-coated sections. *In situ* hybridization for HPRT mRNA was performed using ^{35}S-labeled riboprobes; the sections were counterstained with cresyl violet, coated with Kodak NTB-2 photographic emulsion, exposed for 7–10 days, and developed. Silver grains showing areas of probe hybridization are represented

by adenosine deaminase (ADA) and/or purine nucleoside phosphorylase (PNP) to inosine and hypoxanthine. This second route of metabolism requires the presence of HPRT for reincorporation of these metabolites into the utilizable purine pools (the ADA–PNP–HPRT pathway), and the absence of HPRT may cause a continual depletion of purines from cells that depend heavily on this route of metabolism. The involvement of both AK and ADA in the metabolism of purines in the brain has been demonstrated in synaptosomal preparations (50–53), slices or dissected regions of brain tissue *in vitro* (50, 54–57), and neurons and glia in tissue culture (58–60). In fact, previous studies have shown that cultures of purified glial cells metabolize free adenosine predominantly by the AK pathway, while cultured neurons appear to depend more heavily on the ADA–PNP–HPRT pathway (60). The differences in the relative usage of AK or ADA for adenosine metabolism by neurons and glia may explain the higher requirement for HPRT in some neurons.

Whether there is any functional relationship between HPRT and the purine neurotransmitter systems remains to be established, but it is intriguing that, as shown for HPRT in the current study, several "housekeeping" enzymes involved in purine metabolism such as ADA, PNP, and 5′-nucleotidase show highly specific patterns of localization in the brain (61–69). Curiously, the neuroanatomical patterns of expression of these enzymes demonstrate no obvious concordance. The lack of obvious overlap in the distribution of these enzymes suggest that different purines or different routes of metabolism play specialized roles in different brain subregions or that these enzymes are involved in other, as yet unidentified, functions. The involvement of potential markers of purine neurotransmitter systems in intermediate purine metabolism, together with uncertainties regarding which purines function as neurotransmitters in which brain regions, has made it difficult to produce a definitive neuroanatomical map of purine neurotransmitter systems in the brain.

In addition to its potential role in purine-related neurotransmission, regional differences in the expression of HPRT may also reflect its role in receptor-mediated signal transduction mechanisms involving purines. A wide variety of neurotransmitter, neuropeptide, and hormone receptors use the purines cyclic adenosine monophosphate (cAMP) or cyclic guanine monophosphate (cGMP) as intracellular messengers for signal transduction (70–74). These receptors, as well as other receptors, require additional membrane proteins (G proteins) whose function depends on the availability of guanosine triphosphate (GTP), another purine. It has been previously postulated that, although HPRT is not directly involved in the metabolism of cyclic nucleotides or GTP, the absence of HPRT may be associated with consequences of purine metabolism that affect these signal transduction systems indirectly (75–77). The involvement of HPRT in these processes remains unclear as little information concerning signal transduction in HPRT-deficient cells is currently available. However, with the availability of HPRT-mice, it may be possible to determine whether HPRT plays a role in these processes.

The distribution of HPRT mRNA shown in Fig. 4 demonstrates no obvious relationship to that described for any of the other widely studied neurotransmitter systems, including dopamine, norepinephrine, serotonin, acetylcholine, or GABA. Nevertheless, in HPRT-deficient humans and mice, the occurrence of specific abnormalities of dopamine systems suggests that HPRT might play an important role in the normal functioning of the dopaminergic systems (12–15). This suggestion is supported by the finding in the human brain that the basal ganglia contain the highest levels of HPRT activity in the brain (1–3). However, our *in situ* hybridization results in the mouse demonstrate moderate levels of HPRT mRNA in regions containing dopamine neurons, such as the substantia nigra and ventral tegmental area, and very low levels in the caudoputamen and accumbens. Thus in the mouse, the major brain dopamine systems and their main target regions do not express particularly high levels of HPRT mRNA.

Several possibilities could account for the dopamine-related abnormalities in HPRT-deficient mice. First, although the mRNA for HPRT does not appear to be preferentially expressed in either the neurons or targets of the dopamine system, it is possible that the HPRT protein is specifically transported via axons or dendrites to synapses in these regions. This suggestion is supported by studies showing that HPRT activity is slightly higher in synaptosomal fractions than in cytosolic fractions prepared from the rat brain (78). However, it seems unlikely that the small enrichment of HPRT activity in synaptosomes (less than twofold) could result in any major differences between the localization of HPRT mRNA and HPRT enzyme activity. A second possibility is that there

by black dots, and counterstained cells are identified by a more diffuse grey or black staining. Each panel contains an arrow indicating a neuron with a high silver grain density, and an asterisk to the left of a counterstained cell with few or no silver grains. (A) Neurons of the lateral vestibular nucleus. (B) Motor neurons of the cranial nerve V (trigeminal). (C) Neurons of the trapezoid nucleus surrounded by fibers of the pyramidal tracts. (D) A clearly labeled single Purkinje cell, with modest labeling of the granule and molecular layers. (E) Gigantocellular reticular neurons of the brain stem. (F) Three heavily labeled neurons of the red nucleus.

may be differences in the translation of HPRT mRNA or the stability of the HPRT enzyme in different regions of the brain. To date, there is no evidence for differential regulation of HPRT mRNA translation or protein stability in different brain regions. A third possibility is that HPRT is expressed at high levels in dopamine-rich brain regions during a critical developmental stage, and the absence of HPRT disrupts normal development of these regions. A final possibility is that the dopamine systems are much more vulnerable to the pathophysiologic effects of HPRT deficiency than other neuronal systems, irrespective of their levels of HPRT mRNA or enzyme activity.

In summary, *in situ* hybridization studies demonstrate a substantial variation in the regional brain levels of HPRT mRNA. In general, neurons express considerably more HPRT than glia, suggesting that HPRT plays a particularly important role in neuronal function. Importantly, these results do not confirm the expectation of high levels of HPRT in the basal ganglia. In addition to documenting the normal pattern of HPRT expression in the mouse brain, the current studies demonstrate the absence of detectable HPRT mRNA in the brains of the $HPRT^-$ mice. Thus these mice offer a unique tool for exploring the role of HPRT in neurological function.

ACKNOWLEDGMENTS

We thank Dr. David Whittingham (MRC Experimental Embryology and Teratology Unit, St. George's Hospital Medical School, London) for supplying us with the HPRT-deficient strain of mice. This work was supported by the Medical Scientist Training Program grant to UCSD (H.A.J.), the American Epilepsy Society (E.J.H.), NIH Grant HD20034-07 (T.F.), and NIH Grant NS23038 (M.C.W.).

REFERENCES

1. Rosenbloom, F. M., W. N. Kelley, J. Miller, J. F. Henderson, and J. E. Seegmiller (1967). Inherited disorder of purine metabolism. *JAMA* **202:** 175–177.
2. Adams, A., and R. A. Harkness (1976). Developmental changes in purine phosphoribosyltransferases in human and rat tissues. *Biochem. J.* **160:** 565–576.
3. Watts, R. W. E., E. Spellacy, D. A. Gibbs, J. Allsop, R. O. McKeran, and G. E. Slavin (1982). Clinical, post-mortem, biochemical and therapeutic observations on the Lesch–Nyhan syndrome with particular reference to the neurological manifestations. *Q. J. Med.* **201:** 43–78.
4. Krenitsky, R. A. (1969). Tissue distribution of purine ribosyl- and phosphoribosyltransferases in the rhesus monkey. *Biochem. Biophys. Acta* **179:** 506–509.
5. Murray, A. W. (1966). Purine-phosphoribosyltransferase activities in rat and mouse tissues and in Ehrlich ascites-tumor cells. *Biochem. J.* **100:** 664–670.
6. Lo, Y. V., and M. Palmour (1979). Developmental expression of murine HPRT. I. Activities, heat stabilities, and electrophoretic mobilities in adult tissues. *Biochem. J.* **17:** 737–746.
7. Lesch, M., and W. L. Nyhan (1964). A familial disorder of uric acid metabolism and central nervous system function. *Am. J. Med.* **36:** 561–570.
8. Seegmiller, J. E., F. M. Rosenbloom, and W. N. Kelley (1967). Enzyme defect associated with a sex-linked hyman neurological disorder and excessive purine synthesis. *Science* **155:** 1682–1684.
9. Nyhan, W. L. (1973). The Lesch–Nyhan syndrome. *Annu. Rev. Med.* **24:** 41–60.
10. Emmerson, B. T., and L. Thompson (1973). The spectrum of hypoxanthine–guanine phosphoribosyltransferase deficiency. *Q. J. Med.* **166:** 423–440.
11. Mizuno, T. (1986). Long-term follow-up of ten patients with Lesch–Nyhan syndrome. *Neuropediatrics* **17:** 158–161.
12. Lloyd, K. G., O. Hornykiewicz, L. Davidson, K. Shannak, I. Farley, M. Goldstein, M. Shibuya, W. N. Kelley, and I. H. Fox (1981). Biochemical evidence of dysfunction of brain neurotransmitters in the Lesch–Nyhan syndrome. *N. Engl. J. Med.* **305:** 1106–1111.
13. Baumeister, A. A., and G. D. Frye (1985). The biochemical basis of the behavioral disorder in the Lesch–Nyhan syndrome. *Neurosci. Biobehav. Rev.* **9:** 169–178.
14. Silverstein, F. S., M. V. Johnston, R. J. Hutchinson, and N. L. Edwards (1985). Lesch–Nyhan syndrome: CSF neurotransmitter abnormalities. *Neurology* **35:** 907–911.
15. Jankovic, J., C. T. Caskey, J. T. Stout, and I. J. Butler (1988). Lesch–Nyhan syndrome: A study of motor behavior and cerebrospinal fluid neurotransmitters. *Ann. Neurol.* **23:** 466–469.
16. Alpin, R. L., A. B. Young, and J. B. Penney (1987). The functional anatomy of basal ganglia disorders. *Trends Neurosci.* **12:** 366–375.
17. Hooper, M., K. Hardy, A. Handyside, S. Hunter, and M. Monk (1987). HPRT-deficient (Lesch–Nyhan) mouse embryos derived from germline colonization by cultured cells. *Nature* **326:** 292–295.
18. Kuehn, M. R., A. Bradley, E. J. Robertson, and M. J. Evans (1987). A potential animal model for Lesch–Nyhan syndrome through introduction of HPRT mutations into mice. *Nature* **326:** 295–298.
19. Jinnah, H. A., F. H. Gage, and T. Friedmann (1991). Amphetamine-induced behavioral phenotype in a hypoxanthine–guanine phosphoribosyltransferase-deficient mouse model of Lesch–Nyhan syndrome. *Behav. Neurosci.* **105:** 1004–1012.
20. Jinnah, H. A., T. Page, and T. Friedmann (1991). Inherited impairment of purine recycling in the mouse: Consequences for brain purine and dopamine systems. *Soc. Neurosci. Abstr.*
21. Williamson, D. J., J. Sharkey, A. R. Clarke, A. Jamieson, G. W. Arbuthnott, P. A. T. Kelley, D. W. Melton, and M. L. Hooper (1991). Analysis of forebrain dopaminergic pathways in HPRT- mice. In *Purine and Pyrimidine Metabolism in Man,* Vol VII, in press.
22. Dunnett, S. B., and D. J. S. Sirinathsinghji (1989). Monoamine deficiency in a transgenic (Hprt-) mouse model of Lesch–Nyhan syndrome. *Brain Res.* **501:** 401–406.
23. Finger, S., R. P. Heavens, D. J. S. Sirinathsinghji, M. R. Kuehn, and S. B. Dunnett (1988). Behavioral and neurochemical evaluation of a transgenic mouse model of Lesch–Nyhan syndrome. *J. Neurol. Sci.* **86:** 203–213.
24. Page, T. M., R. L. Broock, W. L. Nyhan, and L. H. Nieto (1986). Use of selective media for distinguishing variant forms of hypoxanthine phosphoribosyl transferase. *Clin. Chim. Acta* **154:** 195–202.
25. Sambrook, J., E. F. Fritsch, and T. Maniatis (1989). *Molecular Cloning: A Laboratory Manual,* 2nd ed. Cold Spring Harbor Laboratory Press, Cold Spring Harbor, NY.
26. Konecki, D. S., J. Brennand, J. C. Fuscoe, C. T. Caskey, and A. C. Chinault (1982). Hypoxanthine–guanine phosphoribosyltransferase genes of mouse and Chinese hamster: Construction and sequence analysis of cDNA recombinants. *Nucleic Acids Res.* **10:** 6763–6775.

27. Chomczynski, P., and N. Sacchi (1987). Single-step method of RNA isolation by acid guanidinium thiocyanate–phenol–chloroform extraction. *Anal. Biochem.* **162:** 156–159.
28. Danielson, P. E., S. Forss-Petter, M. A. Brow, L. Calavetta, J. Douglass, R. J. Milner, and J. G. Sutcliffe (1988). p1B15: A cDNA clone of the rat mRNA encoding cyclophilin. *DNA* **7:** 261–267.
29. Dush, M. K., J. M. Sikela, S. A. Khan, J. A. Tischfield, and P. J. Stambrook (1985). Nucleotide sequence and organization of the mouse adenine phosphoribosyltransferase gene: Presence of a coding region common to animal and bacterial phosphoribosyltransferases that has a variable intron/exon arrangement. *Proc. Natl. Acad. Sci. USA* **82:** 2731–2735.
30. Cleveland, D. W., M. A. Lopata, R. J. MacDonald, N. J. Cowan, W. J. Rutter, and M. W. Kirschner (1980). Number and evolutionary conservation of α- and β-tubulin and cytoplasmic β- and γ-actin genes using specific cloned cDNA probes. *Cell* **20:** 95–105.
31. Wilson, W. C., and G. A. Higgins (1989). In situ hybridization. In *Neuromethods: Molecular Neurobiological Techniques* (A. A. Boulton, G. B. Baker, and A. T. Campagnoni, Eds.), Vol. 16, pp. 239–284. Humana Press, Clifton, NJ.
32. Thompson, S., A. R. Clarke, A. M. Pow, M. L. Hooper, and D. W. Melton (1989). Germ line transmission and expression of a corrected HPRT gene produced by gene targeting in embryonic stem cells. *Cell* **56:** 313–321.
33. Stout, J. T., and C. T. Caskey (1985). HPRT: Gene structure, expression, and mutation. *Annu. Rev. Genet.* **19:** 127–148.
34. Melton, D. W. (1987). HPRT gene organization and expression. *Oxford Surv. Eukaryotic Genes* **4:** 35–75.
35. Lad, R. P., M. A. Smith, and D. C. Hilt (1991). Molecular cloning and regional distribution of rat brain cyclophilin. *Mol. Brain Res.* **9:** 239–244.
36. Mita, S., E. A. Schon, and J. Herbert (1989). Widespread expression of amyloid beta-protein precursor gene in rat brain. *Am. J. Pathol.* **134:** 1253–1261.
37. Oyler, G. A., G. A. Higgins, R. A. Hart, E. Battenberg, M. Billingsley, F. E. Bloom, and M. C. Wilson (1989). The identification of a novel synaptosomal-associated protein, SNAP-25, differentially expressed by neuronal subpopulations. *J. Cell Biol.* **109:** 3039–3051.
38. Trimble, W. S., T. S. Gray, L. A. Elferink, M. C. Wilson, and R. H. Scheller (1990). Distinct patterns of expression of two VAMP genes within the rat brain. *J. Neurosci.* **10:** 1380–1387.
39. Lewis, S. A., and N. J. Cowan (1985). Temporal expression of mouse glial fibrillary acidic protein mRNA studied by a rapid in situ hybridization procedure. *J. Neurochem.* **45:** 913–919.
40. Landry, C. F., G. O. Ivy, and I. R. Brown (1990). Developmental expression of glial fibrillary acidic protein mRNA in the rat brain analyzed by in situ hybridization. *J. Neurosci. Res.* **25:** 194–203.
41. Verity, A. N., and A. T. Campagnoni (1988). Regional expression of myelin protein genes in the developing mouse brain: In situ hybridization studies. *J. Neurosci. Res.* **21:** 238–248.
42. Shiota, C., M. Miura, and K. Mikoshiba (1989). Developmental profile and differential localization of mRNAs of myelin protein (MBP and PLP) in oligodendrocytes in the brain and in culture. *Dev. Brain. Res.* **45:** 83–94.
43. Kristensson, K., N. K. Zeller, M. E. Dubois-Dalcq, and R. A. Lazzarini (1986). Expression of myelin basic protein gene in the developing rat brain as revealed by in situ hybridization. *J. Histochem. Cytochem.* **34:** 467–473.
44. Higgins, G. A., H. Schmale, F. E. Bloom, M. C. Wilson, and R. J. Milner (1989). Cellular localization of 1B236/myelin-associated glycoprotein mRNA during rat brain development. *Proc. Natl. Acad. Sci. USA* **86:** 2074–2078.
45. Stone, T. W. (1981). Physiological roles for adenosine and adenosine 5′-triphosphate in the nervous system. *Neuroscience* **6:** 523–555.
46. Dunwiddie, T. V. (1985). The physiological role of adenosine in the central nervous system. *Int. Rev. Neurobiol.* **27:** 63–139.
47. Phillis, J. W., and P. H. Wu (1981). The role of adenosine and its nucleotides in central synaptic transmission. *Prog. Neurobiol.* **16:** 187–239.
48. Snyder, S. H. (1985). Adenosine as a neuromodulator. *Annu. Rev. Neurosci.* **8:** 103–124.
49. Burnstock, G. (1990). Overview: Purinergic mechanisms. In *Biological Effects of Extracellular ATP and Nucleotides* (G. Dubyak and J. S. Fedan, Eds.), pp. 1–17. N.Y. Acad. Sci., New York.
50. Wu, P. H., and J. W. Phillis (1984). Uptake by central nervous tissues as a mechanism for the regulation of extracellular adenosine concentrations. *Neurochem. Int.* **6:** 613–632.
51. Kuroda, Y., and H. McIlwain (1974). Uptake and release of [^{14}C]adenine derivatives at beds of mammalian cortical synaptosomes in a superfusion system. *J. Neurochem.* **22:** 691–699.
52. Daval, J. L., and C. Barberis (1981). Release of radiolabelled adenosine derivatives from superfused synaptosome beds. *Biochem. Pharmacol.* **30:** 2559–2567.
53. Bender, A. S., P. H. Wu, and J. W. Phillis (1980). The characterization of [^{3}H]adenosine uptake into rat cerebral cortical synaptosomes. *J. Neurochem.* **35:** 629–640.
54. Shimizu, H., S. Tanaka, and T. Kodama (1972). Adenosine kinase of mammalian brain: Partial purification and its role for the uptake of adenosine. *J. Neurochem.* **19:** 687–698.
55. Whittingham, T. S., E. Warman, H. Assaf, T. J. Sick, and J. C. LaManna (1989). Manipulating the intracellular environment of hippocampal slices: pH and high-energy phosphates. *J. Neurosci. Methods* **28:** 83–91.
56. Santos, J. N., K. W. Hempstead, L. E. Kopp, and R. P. Miech (1968). Nucleotide metabolism in rat brain. *J. Neurochem.* **15:** 367–376.
57. Wong, P. C. L., and J. F. Henderson (1972). Purine ribonucleotide biosynthesis, interconversion and catabolism in mouse brain in vitro. *Biochem. J.* **129:** 1085–1094.
58. Hertz, L. (1978). Kinetics of adenosine uptake into astrocytes. *J. Neurochem.* **31:** 55–62.
59. Meghji, P., J. B. Tuttle, and R. Rubio (1989). Adenosine formation and release by embryonic chick neurons and glia in cell culture. *J. Neurochem.* **53:** 1852–1860.
60. Matz, H., and L. Hertz (1989). Adenosine metabolism in neurons and astrocytes in primary cultures. *J. Neurosci. Res.* **24:** 260–267.
61. Nagy, J. I., L. A. LaBella, and M. Buss (1984). Immunohistochemistry of adenosine deaminase: Implications for adenosine neurotransmission. *Science* **224:** 166–168.
62. Staines, W. A., P. E. Daddona, and J. I. Nagy (1987). The organization and hypothalamic projections of the tuberomammillary nucleus in the rat: An immunohistochemical study of adenosine deaminase-positive neurons and fibers. *Neuroscience* **2:** 571–596.
63. Miguel-Hidalgo, J. J., E. Senba, S. Matsutani, K. Takatsuji, and M. Tohyama (1989). Adenosine deaminase containing fiber pathway from the superior colliculus to the lateral posterior nucleus of the rat. *Brain Res.* **476:** 189–193.
64. Yamamoto, T., W. A. Staines, K. Dewar, J. D. Geiger, P. E. Daddona, and J. I. Nagy (1988). Distinct adenosine deaminase-containing inputs to the substantia nigra from the striatum and tuberomammillary nucleus. *Brain Res.* **474:** 112–124.
65. Van Reempts, J., B. Van Deuren, M. Haseldonckx, M. Van de Ven, F. Thone, and M. Borgers (1988). Purine nucleoside phosphorylase: A histochemical marker for glial cells. *Brain Res.* **462:** 142–147.

66. Scott, T. G. (1967). The distribution of 5′-nucleotidase in the brain of the mouse. *J. Comp. Neurol.* **129:** 97–114.

67. Cammer, W., R. Sacchi, and S. Kahn (1985). Immunocytochemical localization of 5′-nucleotidase in oligodendroglia and myelinated fibers in the central nervous system of adult and young rats. *Dev. Brain. Res.* **20:** 89–96.

68. Schoen, S. W., M. B. Graeber, M. Reddington, and G. W. Kreutzberg (1987). Light and electron microscopical immunocytochemistry of 5′-nucleotidase in rat cerebellum. *Histochemistry* **87:** 107–113.

69. Bernstein, H. G., J. Weib, and H. Luppa (1978). Cytochemical investigations on the localization of 5′-nucleotidase in the rat hippocampus with special reference to synaptic regions. *Histochemistry* **55:** 261–267.

70. Garbers, D. L. (1990). The guanylyl cyclase receptor family. *New Biol.* **2:** 499–504.

71. Goy, M. F. (1991). cGMP: The wayward child of the cyclic nucleotide family. *Trends Neurosci.* **14:** 293–299.

72. Birnbaumer, L. (1990). G-proteins in signal transduction. *Annu. Rev. Pharmacol. Toxicol.* **30:** 675–705.

73. Ross, E. M. (1989). Signal sorting and amplification through G protein-coupled receptors. *Neuron* **3:** 141–152.

74. Gilman, A. G. (1987). G proteins: Transducers of receptor-generated signals. *Annu. Rev. Biochem.* **56:** 615–649.

75. Watts, R. W. E. (1985). Defects of tetrahydrobiopterin synthesis and their possible relationship to a disorder of purine metabolism (the Lesch–Nyhan Syndrome). *Adv. Enzyme Regul.* **23:** 25–58.

76. Goldstein, M., L. T. Anderson, R. Reuben, and J. Dancis (1985). Self-mutilation in Lesch–Nyhan disease is caused by dopaminergic denervation. *Lancet* **1:** 338–339.

77. Goldstein, M. (1989). Monkeys with unilateral ventromedial tegmental lesions of the brain stem: Model for Parkinson's disease and Lesch–Nyhan syndrome. *Prog. Neuro-Psychopharmacol. Biol. Psychiatry* **13:** 311–318.

78. Gutensohn, W., and G. Guroff (1972). Hypoxanthine–guanine phosphoribosyltransferase from rat brain (purification, kinetic properties, development and distribution). *J. Neurochem.* **19:** 2139–2150.